JOURNAL OF MATERIALS SCIENCE 19 (1984) 1099–1108

Nitrocarburizing of low-carbon unalloyed steel

Part 2 *Positron annihilation studies*

S. DANNEFAER, B. HOGG, D. KERR
Department of Physics, University of Winnipeg, Winnipeg, R3B 2E9, Canada

Low-carbon unalloyed steel has been investigated after nitriding accomplished by either the salt-bath method (Tenifer) or the gas method (Nitroc). The resulting changes in the position annihilation parameters are reported in this paper, while changes in the mechanical properties are reported in the preceding paper. The positron lifetime measurements show that small vacancy clusters in which the positron lifetime is ~ 240 psec are present in the steel and that they are thermally stable even up to 570° C. A fast cooling from this temperature appears to freeze in monovacancy–impurity complexes. Positrons annihilating in the surface layer (formed by the nitriding processes and consisting of $Fe_{2-3}N$) reveal that a high concentration of large vacancy clusters can be present in the outermost 4 μm of this layer. The Tenifer treatment appears to result in the presence of more clusters than in the Nitroc treatment. The positron lifetime in these clusters is ~ 300 psec and this component disappears upon annealing at 100° C. Positrons annihilating in the diffusion zone below the surface layer indicate that dislocations are created around $Fe_{16}N_2$ and Fe_4N precipitates. The interpretation of the positron data provides a physical understanding of the mechanical data presented in the preceding paper.

1. Introduction

An investigation of the mechanical properties of nitrided steel is described in the preceding paper "Nitrocarburizing of Low-Carbon Unalloyed Steel Part 1: Mechanical Properties", hereafter referred to as Part 1. In this second part, we present the results of positron annihilation measurements on the same set of specimens, i.e. salt-bath nitrided (Tenifer process) and gas nitrided (Nitroc process) tensile bars which were subjected to various degrees of elongation and annealing. The positron measurements were performed in an attempt to understand the atomic mechanism responsible for the macroscopic properties resulting from nitriding. To review briefly the fundamentals of the nitriding process, exposure to a nitrogen compound results in a thin surface layer containing a high concentration of nitrogen as $Fe_{2-3}N$, and an extended diffusion zone with a much lower concentration of nitrogen as precipitates of $Fe_{16}N_2$ or Fe_4N.

The positron annihilation technique has been used for several years in the laboratory to investigate the basic properties of defects in solids and has been reviewed by Hautojärvi [1] and West [2]. However, only recently has there been sufficient fundamental knowledge to facilitate investigations of the more complex materials of engineering importance [3–7].

The singular property of positrons which makes them suitable for studies of metals (or materials in general) is their extreme sensitivity to defects such as vacancies and dislocations. This stems from the fact that, in general, a positron will seek an "empty" space in the material, thereby lowering its total energy. As a consequence of the trapping in vacancy-like areas, the positron will sample a lower electron density, which in turn means that the lifetime of such a trapped positron will be longer than the lifetime of an untrapped positron. As an example, with relevance to the present work,

0022–2461/84 $03.00 + .12

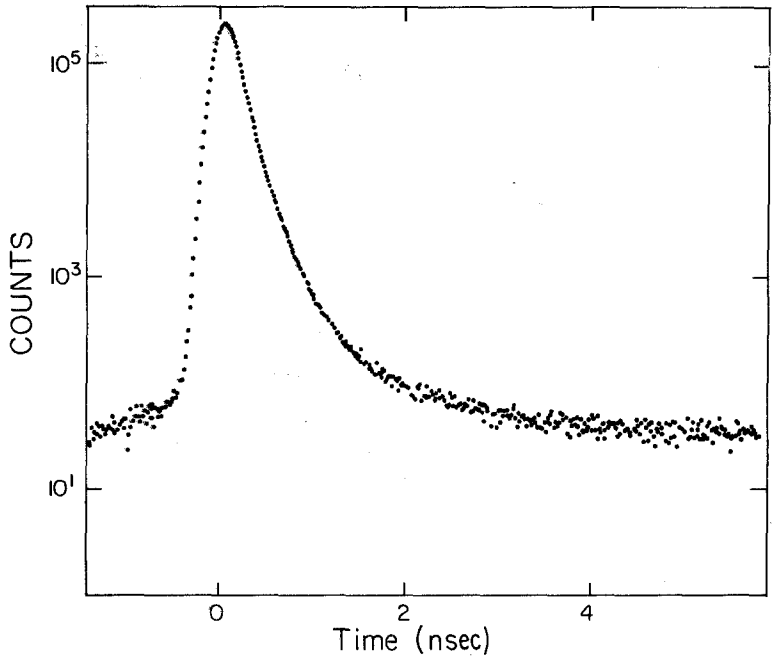

Figure 1 Lifetime spectrum for a nitrided iron sample. The spectrum contains a total of 5×10^6 counts.

Vehanen *et al.* [8] have shown that positrons in perfect (i.e. defect-free) iron has a characteristic lifetime of 110 psec while a positron trapped in a monovacancy has a lifetime of about 175 psec. They have further shown that when monovacancies form voids (too small to be observed by electron microscopy) the lifetime of positrons trapped in these voids increases to a value of about 350 psec. This example shows that the positron annihilation method yields information on defect structures down to the monovacancy level. We will return to some further details of the method at the end of the next section.

2. Experimental details

Samples for the positron measurements were cut from the centre portion of tensile bars identical to those used for the mechanical testing (Part 1) and the positron source was placed between two identical sample pieces. The positron source consisted of 7 μCi of ^{22}NaCl deposited onto a thin (1 μm) aluminium foil and yielded a coincidence count rate of 150 counts per second.

Positron lifetime spectra were obtained using slightly tapered $1\frac{1}{2}$ in. $\times$ $1\frac{1}{2}$ in. Pilot U scintillators coupled to RCA 8575 photomultipliers to measure the time difference between the nuclear gamma ray associated with positron emission and one of the annihilation gamma rays. The scintillators were polished but no reflecting paint was applied to their surfaces to ensure a minimum time spread of the light pulses [9]. The resulting time resolution under actual operating conditions was 290 $\pm$ 3 psec (full width at half maximum). The ^{22}Na energy windows in the fast-fact coincidence spectrometer were chosen such that the backscattering contribution to the lifetime spectra was less than 0.6% [10]. Each lifetime spectrum consisted of $\sim 5 \times 10^6$ events and all measurements were performed at room temperature.

The lifetime spectra, an example of which is shown in Fig. 1, were analysed according to the following mathematical model:

$$n(t) = \sum_{i=1}^{m} I_i \exp(-t/\tau_i) \qquad (1)$$

where I_i denotes the intensity of the ith lifetime component characterized by the lifetime, τ_i, and $\Sigma_{i=1}^{m} I_i = 1$. It will be shown later that the shortest lifetime, τ_1, is associated with the annihilation of positrons in a defect-free part of the sample while the longer lifetimes τ_2, τ_3 etc. are related to positrons annihilating in various defects. Further, the corresponding intensities I_2, I_3 etc. are related to the fraction of positrons trapped by these defects. The actual analysis of the spectra was done using the computer programmes Resolution and Positronfit [11]. The contribution to the lifetime spectra from annihilations in the aluminium foil and the ^{22}NaCl itself was determined as described

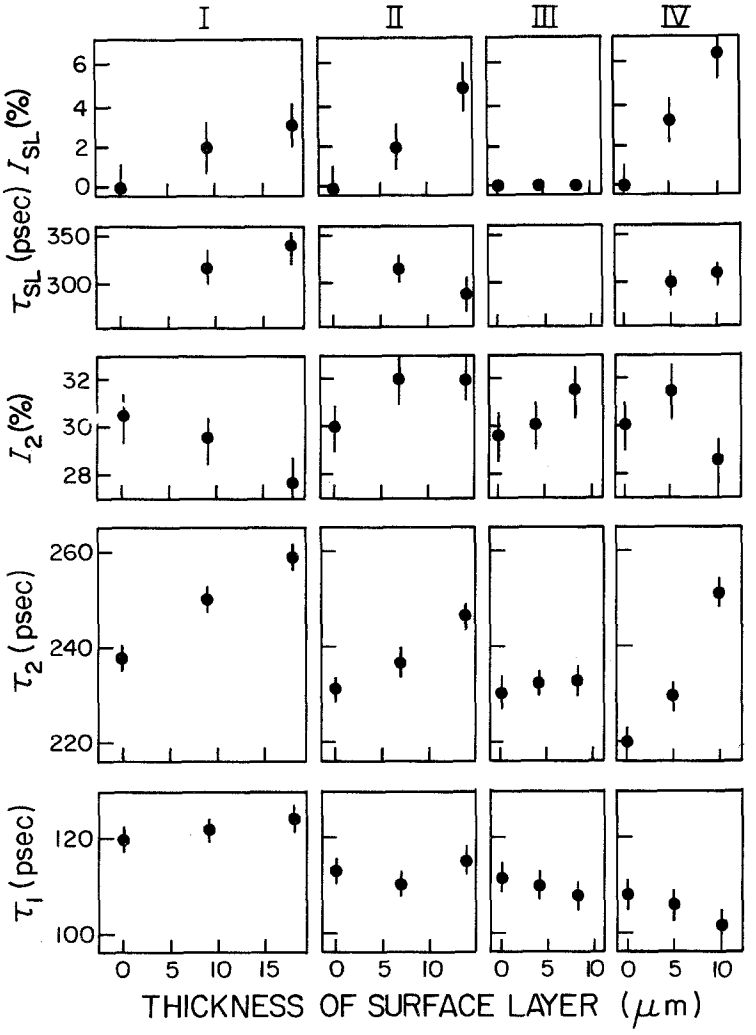

Figure 2 Lifetime results for various thicknesses of surface layers. Columns I, II and III: Nitroc-treated with surface layer thicknesses 18, 14 and 8 μm. Column IV: Tenifer-treated, 10 μm surface layer thickness. τ_1, τ_2 and I_2 are the results for two-term fits. τ_{SL} and I_{SL} are the results for the surface layer only. The pre-strain value was 0%.

in reference [12] and consisted of a 250 psec component of intensity 2.3% and an 860 psec component of intensity 0.9%.

In performing the measurements on the nitrided samples, it was necessary to take account of the fact that the positrons would annihilate in two different regions, the surface layer and the diffusion zone. The positron penetration profile is expressed as $e^{-\beta x}$ where $\beta \simeq 250\ cm^{-1}$ for iron [13]. Neglecting the small difference in β for iron and $Fe_{2-3}N$, approximately 20% of the positrons will annihilate in a surface layer having a thickness of 10 μm. Since it is desirable to separate the surface layer and diffusion zone contributions to the lifetime spectra, it was necessary to perform measurements first with the surface layer in place and then with it removed by polishing. The polishing was performed by hand, and since the surface layer had a distinct yellow tinge, it was not difficult to observe when the layer had been removed.

3. Results

Fig. 2 shows the positron annihilation parameters obtained in a series of measurements on gas (Nitroc) and salt-bath (Tenifer) nitrided samples. Three different sets of Nitroc-treated samples were investigated, each having a different surface layer thickness. The different thicknesses were achieved by placing the samples in different locations in the retort used in gas nitriding. The abscissa in this figure indicates the combined surface layer thickness of the two samples surrounding the positron source. The data on the right in each panel were obtained with both surface layers intact, while the data in the middle and on the left of each panel were obtained with one or both surface layers removed respectively.

The lifetime spectra were first analysed assuming the presence of only two lifetime components yielding the τ_1, τ_2 and I_2 ($I_1 = 100 - I_2$) values in Fig. 2. The data analysis indicated unequivocally the presence of at least two lifetime components and the reduced χ^2 varied between 1.0 and 1.2, displaying no systematic deviation between model and experiment. However, since τ_2 increases with total surface layer thickness for each set of samples, this component must be composite, consisting of lifetimes too close in value to be resolved by the unconstrained computer analysis. However, assuming that the composite nature of this component arises from annihilations in the surface layer and the diffusion zone, the analysis may be carried a step further by noting that the response from the diffusion zone alone (which we denote as τ_1^0, τ_2^0, and I_2^0) is that observed for zero thickness of the surface layer. Lifetime spectra for non-zero surface layer thickness must therefore contain the τ_1^0 and τ_2^0 components but the intensity I_2^0 will not be maintained since some positrons will be stopped in the surface layer. However, the ratio I_1^0/I_2^0 will remain constant regardless of the surface layer thickness. The lifetime spectra for non-zero surface layer thickness were therefore re-analysed employing the above constraints and allowing an additional unconstrained lifetime component to account for annihilations in the surface layer itself. This component is characterized by the lifetime τ_{SL}, and the intensity I_{SL}, shown at the top of the panels in Fig. 2. The reduced χ^2 values were similar to those obtained in the previous analysis and no more than one additional lifetime could be resolved.

It is apparent that τ_{SL} is roughly constant and is, as expected from the behaviour of τ_2, larger than the τ_2^0 values. I_{SL} increases linearly with thickness although the values are unexpectedly small in view of the fraction of positrons annihilating in the surface layer. It is noteworthy that in one case, namely for the rather thin surface layer of 8 μm, no τ_{SL} component could be detected, that is the lifetime spectra with and without an 8 μm surface layer were identical.

The measurements described in connection with Fig. 2 were all performed on samples cut from bars that had not been subjected to any deformation prior to nitriding. Similar measurements were also carried out for samples cut from bars which had received 1.3%, 5% and 20% tensile deformation prior to the nitriding process which produced a surface layer of approximately 10 μm thickness in all cases. The annihilation parameters obtained after removal of the surface layers from the nitrided samples are shown as a function of pre-strain value in Fig. 3. The leftmost panel contains the results for the references for the Nitroc-treated samples (i.e. samples subjected to the same heat treatment as the gas nitrided samples). In the next panel, the results for the Nitroc-treated samples are shown. Note that the I_2^0, τ_1^0 and τ_2^0 values refer to zero thickness of the surface layer, thus facilitating a direct comparison between the references and the nitrogen-loaded diffusion zone. Application of the procedure described above to determine τ_{SL} and I_{SL} yielded surface layer results as indicated. Similar procedures gave results for the Tenifer-treated samples and related references as indicated in the two remaining panels.

Since detailed discussion of these data will be presented in the following section, it suffices to note here that I_{SL} is apparently independent of the pre-strain level and that only the Tenifer-treated samples exhibit changes in I_2^0 and τ_2^0 as a consequence of the nitriding treatment.

The annealing (or ageing), as described in Part 1, was also investigated by the positron annihilation method. Only the Tenifer-treated tensile bars were investigated, and again, the positron measurements were conducted on both zero-thickness and on the full 10 μm thickness of the surface layer. The results are shown in Fig. 4, where τ_1^0, τ_2^0 and I_2^0 are the lifetimes for zero thickness of the surface layer and I_{SL} is the intensity of the surface component. Non-zero values of I_{SL} were only observed for $T = 20^\circ$ C and 60° C while at higher annealing temperatures, the lifetime spectra with and without a surface layer were identical. The temperature range in which τ_2^0 changes agrees fairly well with the range in which most of the change in σ_{1y} takes place (see Fig. 8, Part 1).

4. Discussion

Since the positron measurements are sensitive to defects on an atomic level, this part of the discussion will begin with a consideration of the possible effects from heat treatment alone, i.e. by considering the reference samples first.

4.1. Non-nitrided samples

In Fig. 3 the results for the non-nitrided samples are shown in the columns denoted RN (reference for Nitroc-treated samples) and RT (reference for

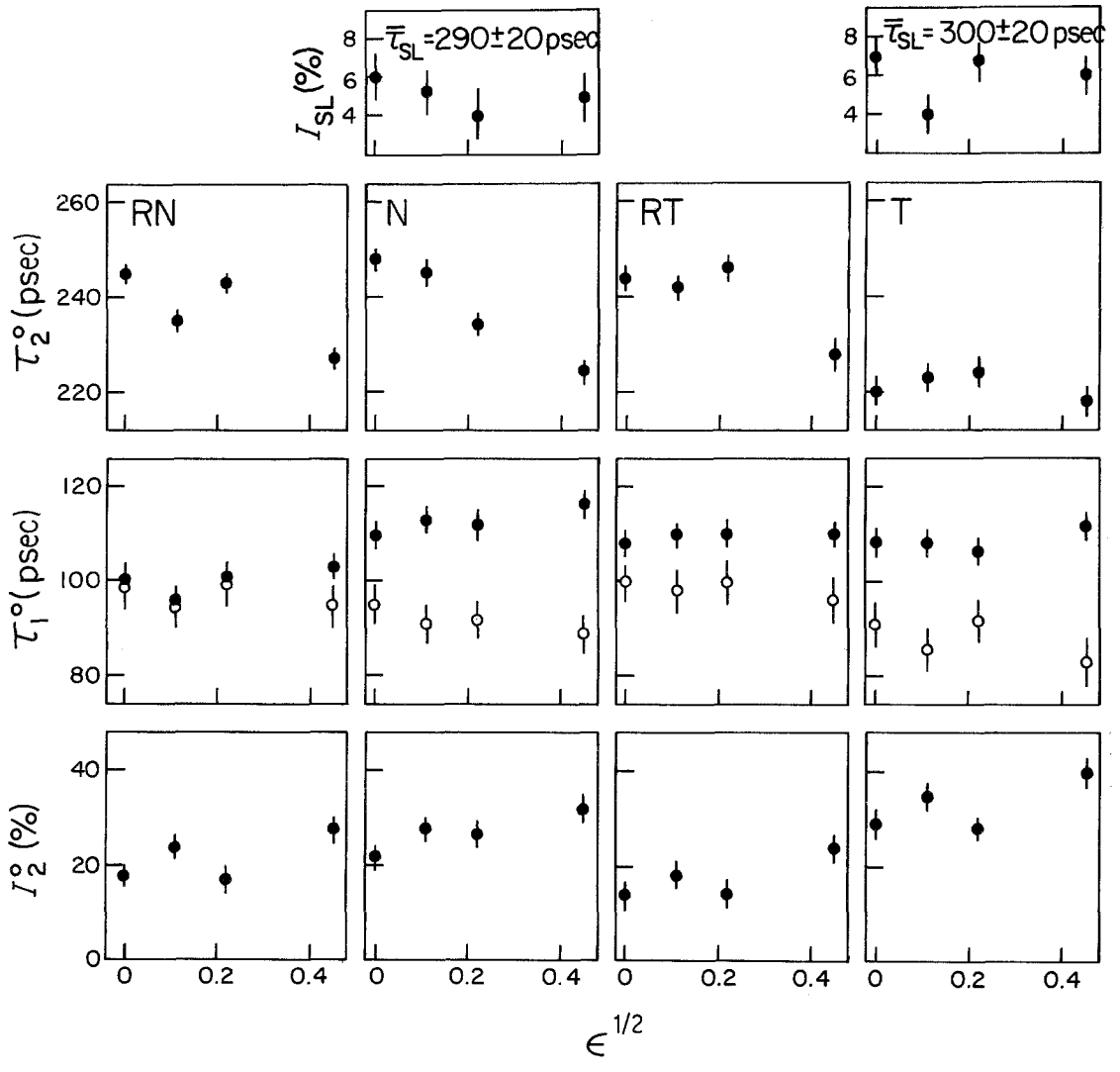

Figure 3 Lifetime results for variously treated samples as a function of the square root of pre-strain, ϵ. The labels RN, N, RT and T denote the reference samples for the Nitroc-treated samples, the Nitroc-treated samples, the references for the Tenifer-treated samples and the Tenifer-treated samples respectively. The data shown in the τ_2^0, τ_1^0 and I_2^0 panels are all for zero thickness of the surface layer. τ_{SL} and I_{SL} are the results for the surface layer only. The open circles in the τ_1^0 panel refer to values calculated using Equation 4.

Tenifer-treated samples). Even for these annealed samples, it is clear that some defects are present simply due to the fact that a long-lived (τ_2^0) component is present in the lifetime spectra. According to the so-called trapping model [2], a positron at time $t = 0$ is assumed to be in a state where it either can annihilate in the perfect lattice or be transferred to various defects in the sample. This results in a lifetime spectrum of the following form:

$$n(t) = \left\{ 1 - \sum_j \frac{K_{1j}}{\lambda_1 - \lambda_j + \Sigma} \right\} \exp\left[-(\lambda_1 + \Sigma)t\right] + \sum_j \frac{K_{1j}}{(\lambda_1 - \lambda_j + \Sigma)} \exp\left(-\lambda_j t\right), \quad j \neq 1. \tag{2}$$

Here λ_1 is the annihilation rate from the perfect lattice, K_{1j} is the transition rate from the initial state to some other state j with the annihilation rate $\lambda_j = 1/\tau_j$, where τ_j is the positron lifetime in the jth defect state. Σ is the sum of all transition rates, i.e. $\Sigma_j K_{1j}$. The rates K_{1j} are proportional to the defect concentrations, C_j. In the present experiment only two lifetimes could be resolved

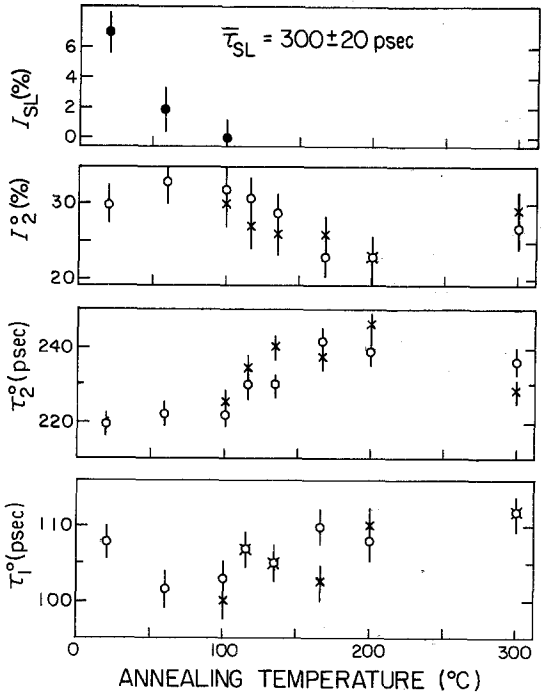

Figure 4 Lifetime results as a function of annealing temperature for Tenifer-treated samples. A new sample was used at each annealing temperature. Crosses and open circles refer to samples with and without the surface layer respectively. τ_{SL} and I_{SL} are the results for the surface layer only. The surface layer thickness was 10 μm and the pre-strain value was 0%.

for the reference samples even though there is undoubtedly more than one type of defect present. This suggests that the individual annihilation rates, λ_j ($j \neq 1$) have very similar values so that an average of the annihilation rates (or lifetimes, τ_j) is being observed. Rewriting Equation 2 for the case of only one defect type yields:

$$n(t) = \left\{1 - \frac{K}{(\lambda_1 - \lambda_2 + K)}\right\} \exp\left[-(\lambda_1 + K)t\right] + \frac{K}{(\lambda_1 - \lambda_2 + K)} \exp(-\lambda_2 t). \quad (3)$$

One may therefore associate the experimentally determined parameter I_2 with $K/(\lambda_1 - \lambda_2 + K)$, τ_1 with $1/(\lambda_1 + K)$, i.e. the inverse of the annihilation rate plus transition rate from the perfect lattice, and τ_2 with $1/\lambda_2$. Since λ_1 can be determined directly from a measurement on defect-free α-iron, one may calculate the value of τ_1 [$= 1/(\lambda_1 + K)$] and compare the result with the measured value. The calculation is performed utilizing the expression

$$K = \frac{I_2}{1 - I_2}(\lambda_1 - \lambda_2) \quad (4)$$

which is obtained from the definition of I_2 above. If only one defect type is present, good agreement between the measured and calculated values of τ_1 should be observed; conversely, a discrepancy indicates the presence of additional lifetime components which have not been resolved by the computer analysis.

Using $\lambda_1 = 9.09\ \text{nsec}^{-1}$ as recently determined by Vehanen *et al.* [8], τ_1 is calculated and plotted in Fig. 3 as open circles in the RN (reference for Nitroc-treatment) and RT (reference for Tenifer treatment) columns. For the three lowest degrees of deformation of the RN samples the agreement is very good, but there is substantial disagreement for the largest deformation and for all of the RT samples. This suggests that the reason for the discrepancies must be sought not only in the amount of deformation, but also in the thermal history of the samples, the difference being that the RT samples were cooled more rapidly than the RN samples.

To proceed, it is therefore necessary to consider in more detail the various defect complexes which may occur in the samples. This consideration is based on the work of Vehanen *et al.* [8] in which α-iron with controlled amounts of carbon (5 ppm, 50 ppm and 750 ppm) was irradiated with electrons at low temperature. It was found that carbon–monovacancy complexes were formed as well as vacancy clusters; the complexes dissociated at approximately 215° C and the vacancy clusters were found to anneal out completely at about 330° C. Deformed pure iron (< 5 ppm carbon) was also investigated showing again the formation of vacancy clusters and their disappearance around 330° C leaving, at higher annealing temperatures, only the response from the remaining dislocations. It was further found that the lifetime of a positron trapped by a monovacancy was 175 psec, a lifetime very similar to the 165 psec lifetime of a positron trapped by a dislocation. The lifetime of positrons trapped by vacancy clusters varied according to the cluster size but was typically in the range 250 to 350 psec.

Turning now to the present experiments, we must associate τ_2 with annihilation in vacancy clusters simply because of its rather large value. We note, however, that our samples were subjected to a thermal annealing at 570° C, a tem-

perature higher than the temperature at which vacancy clusters disappeared in the work of Vehanen *et al.* [8]. This significantly increased thermal stability is not likely to be a result of a high carbon content (~ 1000 ppm) in our samples since no dependence of thermal stability on carbon content up to 750 ppm was observed by Vehanen *et al.* Neither does it appear likely that dislocations could have been the stabilizing agent since Vehanen *et al.* did not observe any difference in cluster stability for deformed samples. It is, of course, quite possible that grain boundaries could stabilize the clusters, but, if such were the case, the probability for trapping in the clusters would be very small. The reason here is that the average distance travelled by a positron before annihilation is of the order 1 μm while the average grain size is about 40 μm.

It is therefore suggested that the impurities present in our commercial iron stabilize the clusters to at least 570° C. Manganese, for example, would be in ample supply (400 to 1000 ppm) and its size is significantly larger than carbon, which did not exhibit a stabilizing effect on the clusters. Phosphorous and sulphur, on the other hand, are not likely candidates, since they preferentially segregate at grain boundaries.

Returning now to the RN column in Fig. 3, it is noted that the three smallest degrees of deformation yield the same values of τ_2^0, τ_1^0, and I_2^0. This simply indicates that these deformations have not introduced new defects to compete significantly with the clusters already present in the undeformed samples. Since there is, in addition, perfect agreement between the observed and calculated τ_1^0 values, we are led to the conclusion that clusters alone are responsible for the trapping. As noted earlier, an unresolved lifetime component would generate a discrepancy between the measured and calculated τ_1^0 values. Thus, in the case of the highest degree of deformation where a discrepancy is apparent, there should be at least one lifetime having an intermediate value between τ_1^0 and τ_2^0 (which would tend to increase τ_1^0 and decrease τ_2^0). Vehanen *et al.* found that dislocations yield a lifetime of approximately 165 psec, which would indeed be impossible to separate from a 100 psec and a 240 psec lifetime [10].

The results for the RT samples are quite similar to those for the RN samples, except for the important feature that the calculated τ_1^0 values now are significantly lower than the observed values. Since the only difference in the thermal history of the two samples is that the RN samples were cooled slowly from 570° C while the RT samples were cooled very rapidly, this must account for the discrepancies. Since vacancy clusters at 570° C are probably in some dynamic equilibrium with monovacancies or monovacancy–impurity complexes, rapid cooling could freeze in such complexes and hence contribute an additional lifetime similar to, but larger than, τ_1^0. Indeed, Vehanen *et al.* found that the carbon–monovacancy complex yielded a lifetime of ~ 160 psec. This complex, or possibly a manganese–monovacancy complex, could therefore be the physical explanation for the discrepancies. It is stable at room temperature but not beyond ~ 215° C, allowing the possibility of its presence in rapidly cooled samples but, significantly, not in slowly cooled samples. As a corollary of this, the values of I_2^0 corresponding to trapping in clusters are, as expected, lower in the RT samples than in the RN samples because of the competition from the impurity–monovacancy traps.

These results have shown that vacancy clusters are present in this commercial low-carbon steel and that they are exceptionally stable due to impurities, possibly manganese. The clusters may very well be the precursors for weak spots in the material, and thus of importance from the point of view of the overall strength and fracture pattern.

4.2. Effects of nitriding

The results for the nitrided samples are shown in columns N (Nitroc) and T (Tenifer) of Fig. 3. Recall that the τ_2^0, τ_1^0 and I_2^0 values correspond to zero-thickness of the surface layer, i.e. these results apply to the diffusion-zone only. The I_{SL} and $\bar{\tau}_{SL}$ values correspond to the response from the surface layer only. Since the penetration profile of the positrons in iron is such that virtually no positrons penetrate deeper than ~ 100 μm, the positrons probe a region in the diffusion zone having essentially constant nitrogen content (according to the hardness profiles shown in Figs. 6 and 7, Part 1).

Comparing now the RN samples with the N samples, there is the suggestion that the introduction of nitrogen in the form of Fe_4N precipitates (see Fig. 13, Part 1) does not greatly alter the lifetime spectra. The clusters seem by and large unaffected by the nitriding, but there

is an increase in τ_1^0. Calculating τ_1 from the trapping model (Equation 3), leads us again to the notion that an unresolved lifetime is present. This lifetime could arise from annihilation in, or close by, the precipitates. However, it will be argued later that such precipitates yield a lifetime which is very close to the value in perfect iron (110 psec) and therefore, annihilation in the precipitates is not likely to produce a discernible contribution. The precipitates however, create dislocations due to their misfit with the remaining lattice [14, 15] which may account for the increase in τ_1^0 since annihilation at dislocations yields a lifetime of 165 psec [8]. The positrons would then sense the presence of the precipitates only in an indirect way.

The results for the Tenifer-treated samples differ significantly from those for the Nitroc-treated samples in that τ_2^0 is much lower than the corresponding values for the RT samples, and I_2^0 is significantly larger. Again, this must be a result of the high cooling rate which would create a high concentration of very small precipitates ($Fe_{16}N_2$ and Fe_4N – see Fig. 9, Part 1). The number of resulting dislocations would therefore be expected to be larger than for the Nitroc-treated samples, yielding a higher intensity of the unresolved lifetime intermediate between τ_1^0 and τ_2^0. In the analysis of the lifetime spectra this would have the net effect of lowering the value of τ_2^0 as compared to both the RT and the N samples, and of course, introducing a large discrepancy between the calculated and observed τ_1^0 (see Fig. 3).

The positron measurements thus indicate that the average dislocation density in the diffusion zone is increased substantially, a conclusion agreeing with the findings of Mittemeijer *et al.* [15]. Physically, this is an expected result, since dislocations would be produced both by the overall concentration gradient of nitrogen as well as by locally distributed dislocations around the precipitates.

4.3. Surface layer effects

As described in the results section, only a single lifetime component associated with the surface layer could be extracted from the spectra and the data are presented in the I_{SL} panels of Fig. 3. For both types of nitriding a fairly long lifetime, $\tau_{SL} \simeq 300$ psec, was found, but with an unexpectedly small intensity. As shown in Fig. 2, this intensity was halved upon removal of the surface layer from one of the samples, but the lifetime stayed constant.

The question now is: does τ_{SL} express the lifetime particular to the chemical compound, $Fe_{2-3}N$, or is it related to defects in the $Fe_{2-3}N$ surface layer? This question can easily be answered by calculating the percentage of positrons annihilating in the surface layer. For an 18 μm thick layer the percentage would be approximately 32% and for a 10 μm thick layer, about 20%, clearly indicating that τ_{SL} is associated with defects in the surface layer. Judging from the τ_{SL} value of 300 psec, the defects are, in all likelihood, vacancy clusters.

The spatial distribution of these vacancy clusters, i.e. their depth dependence, was subsequently investigated. By polishing a set of Tenifer-treated samples in steps of ~ 2 μm, it was found that after removal of ~ 4 μm the τ_{SL} component had disappeared completely leaving a spectrum corresponding to that for the diffusion zone alone. Further surface removal left the lifetime spectrum unchanged. Two important conclusions can be drawn from these observations. First, the defects must be confined to the uppermost 4 μm of the surface layer and, since the percentage of positrons which can possibly be stopped within this distance is $\sim 8\%$ (as compared with 6% annihilating in the clusters), nearly all the positrons are trapped in the defects. This nearly complete trapping shows that the defect concentration must be very large, and is in agreement with the commonly observed presence of porosities as found by optical metallographic examinations.

The second conclusion is that annihilation in the remaining part of the surface layer (amounting to $\sim 12\%$ of the positrons) is indistinguishable from annihilation in the diffusion layer. The implication is that, even though a phase transition occurs at 570° C from α-iron (b c c) to the $Fe_{2-3}N$ phase (h c p), this does not remove the vacancy clusters and neither does it change drastically the dislocation density from that prevailing in the top part of the diffusion zone. From this it follows that the precipitates themselves in the diffusion zone, which consist of either $Fe_{16}N_2$ or Fe_4N, are likely to contribute to the lifetime spectrum in very much the same way as the matrix.

It is of particular interest to note that the τ_{SL}

component was not observed in gas-nitrided samples when the surface layer was only 8 μm thick. This seems to indicate that when nitriding is conducted with a low nitrogen potential, i.e. slow growth rate, the surface layer has a high degree of perfection. Dawes *et al.* [16] have arrived at similar conclusions.

4.4. Annealing of Tenifer-treated samples

We will now turn to the last set of measurements in this work. In Fig. 4 are shown the results for the annealing of Tenifer-treated samples. The samples used here are identical to those used in connection with the investigation of the mechanical properties described in Part 1. Measurements were performed on samples with and without a surface layer. The important feature noted here is that the component, arising from the outermost 4 μm, disappears upon annealing at 100° C, and from that point on, the effect from the surface layer is identical to that for the diffusion layer (in accordance with the findings in the preceeding section). The disappearance of I_{SL} at such low temperatures can only mean that interstitial nitrogen is present in the outermost surface layer, and that it becomes trapped by the vacancy clusters thus rendering them inaccessible to the positrons.

At higher temperatures, τ_2^0 is seen to increase in the range 100 to 160° C, i.e. approaching the τ_2^0 value observed for Nitroc-treated samples (see Fig. 3, Column N for $\epsilon^{1/2} = 0$). Referring to the earlier statement that, in the Tenifer-treated samples, a particularly high concentration of monovacancy–impurity complexes (and dislocations) is retained, this indicates that the complexes anneal out in the range 100 to 160° C. This annealing range is close to the onset of the transition from $Fe_{16}N_2$ to Fe_4N [17] and may therefore suggest that the transformation involves vacancy-assisted migration of nitrogen.

We note also that the annealing stage at 100 to 160° C overlaps the second annealing stage observed in the dilation measurements (Fig. 10, Part 1) and corresponds to the temperature range for which the major recovery of the mechanical properties, i.e. lower yield stress, ultimate tensile stress and elongation to fracture, is observed (see Fig. 8, Part 1). This correlation is expected since the overall coarsening of the precipitates accompanying the $Fe_{16}N_2$ to Fe_4N transition would cause a reduction in the dimensions of the samples and the observed change in the mechanical properties.

Comparing further Fig. 10, Part 1, with the present Fig. 4, the low temperature step in the dilation measurements can be correlated only with the reduction in I_{SL}, i.e. the annealing out of the surface component. Notwithstanding the confinement of the surface component to the outermost 4 μm of surface layer, this correlation may result from a relaxation of the surface layer as the nitrogen is trapped by vacancy clusters.

It should also be pointed out that the standard optical microscopy investigation of nitrided samples (see the micrographs presented in Figs. 9 to 13 in Part 1) do not reveal any changes in the region 100 to 160° C in which most of the important physical changes actually occur. It is only above 200° C that changes are readily observable by optical microscopy.

It has been argued several times that the data are consistent with the suggestion that the iron nitrides contribute with a lifetime very close to the 110 psec value for matrix. This argument can be evaluated by considering the change in the iron concentration among the various iron nitrides. In pure iron (b c c crystal structure) the number of iron ions is 8.3×10^{22} cm^{-3}. In Fe_4N (f c c crystal structure) it is 7.3×10^{22} cm^{-3} and, finally, in $Fe_{2-3}N$ (h c p crystal structure) it is 6.8 to 7.2×10^{22} cm^{-3}. Since the annihilation rate is proportional to the number density of electrons [2], then, taking into account only the iron ions, the lifetime should change from 110 psec for α-iron to 118 psec for $Fe_{16}N_2$, 125 psec for Fe_4N and to between 135 and 128 psec for $Fe_{2-3}N$. Although the real changes may be smaller due to the nitrogen ions, it is still striking that there is no difference, for example, between the τ_1 values in Fig. 4 at $T > 100$° C with and without the surface layer. Since the surface layer would stop about 20% of the positrons, the percentage of positrons annihilating with the τ_1^0 lifetime with the surface layer present is $(1.0 - 0.2)\, I_1^0, \simeq 56\%$. The average short lifetime would therefore be $(20\tau_1' + 56\tau_1^0)/(20 + 56)$ where τ_1' is the predicted lifetime for the various iron nitrides. Inserting the appropriate values yields a result indicating that the presence of the surface layer should consistently increase the observed values by 5 to 7 psec, an increase which would be readily observable. We are therefore led to conclude that the positron lifetime in the iron nitrides is very

nearly the same as the lifetime associated with the matrix. It may be that nitrogen plays a significant role, but it appears more likely that the expansion of the lattice due to the introduction of nitrogen is not uniform since the concentration of nitrogen is quite low. The positron, of course, will seek the high electron density areas, thus tending to minimize changes in the lifetime.

5. Conclusions

This work on the positron annihilation characteristics of nitrided low-carbon unalloyed steel has shown the following (see Part 1 for the mechanical properties):

1. Tensile deformation in the range 0% to 20% does not alter the lifetime spectra significantly either for non-nitrided or for nitrided samples. Vacancy clusters are present in the samples yielding a lifetime of ~ 230 psec, and they have an exceptional thermal stability to at least 570° C. It is suggested that this is due to the presence of manganese in the samples. This suggestion indicates that manganese could be detrimental in the sense of stabilizing "weak spots" inside the material.

2. The cooling rate has a marked influence on the number of monovacancy–impurity complexes, the concentration being the largest for rapid cooling.

3. Dislocations are formed around the precipitates in the diffusion zone, but the precipitates themselves do not contribute measurably to the lifetime spectrum.

4. The surface layer contains many vacancy clusters in the outermost 4 μm, yielding a lifetime of ~ 300 psec, and more clusters are present in salt-bath nitrided samples than in gas nitrided samples. No such vacancy clusters could be detected when the surface layer was only 8 μm thick. The remaining part of the surface layer seems not to yield a lifetime spectrum any different from that for the diffusion zone.

5. Annealing of salt-bath nitrided samples indicated that the vacancy clusters in the outermost 4 μm become filled with nitrogen even below 60° C. Subsequent annealing at higher temperatures showed a reduction in the mean dislocation density due to a coarsening of the precipitates. Coupled herewith may also be a reduction of the frozen-in concentration of monovacancy–impurity complexes.

The conclusions based on the positron experiments agree well with those based on the behaviour of the mechanical properties (Part 1). It should be stressed, however, that the positron measurements have provided information which could not have been obtained by other means.

References

1. P. HAUTOJÄRVI (ed.), "Positrons in Solids" (Springer Verlag, Heidelberg, 1979).
2. R. N. WEST, *Adv. Phys.* **22** (1973) 263.
3. C. F. COLEMAN, A. E. HUGHES, F. A. SMITH and M. J. WEAVER, *NDT International* (1982) 87.
4. D. SEGERS, F. van BRABANDER, L. DORIKENS-VANPRAET and M. DORIKENS, *Appl. Phys.* **A27** (1982) 129.
5. W. B. GAUSTER, W. R. WAMPLER, W. B. JONES and J. A. van den AVYLE, in Proceedings of the 5th International Conference on Positron Annihilation, Japan, April, 1979, edited by R. R. Hasiguti and K. Fujiware (The Japan Institute of Metals, Sendai 980, Japan, 1980) p. 125.
6. K. NISHIWAKI, N. OWADA, K. HINODE, S. TANIGAWA, K. SHIBATA, T. FUJITA and M. DOYAMA, *ibid.* p. 177.
7. M. BERNARDIN, A. DUPASQUIER, A. GALLONE and P. PIZZI, *ibid.* p. 181.
8. A. VEHANEN, P. HAUTOJÄRVI, J. JOHANSSON, J. YLI-KAUPPILA and P. MOSER, *Phys. Rev.* **B25** (1982) 762.
9. M. MOSZYŃSKI, *Nucl. Instrum. Methods* **134** (1976) 77.
10. S. DANNEFAER, *Appl. Phys.* **A26** (1981) 255.
11. P. KIRKEGAARD, M. ELDRUP, M. MOGENSEN and N. J. PEDERSEN, *Comp. Phys. Commun.* **23** (1981) 307.
12. S. DANNEFAER, *J. Phys. C: Solid State Phys.* **15** (1982) 599.
13. W. BRANDT and P. PAULIN, *Phys. Rev.* **B15** (1977) 2511.
14. K. YAMAKAWA and F. E. FUJITA, *Met. Trans.* **9A** (1978) 91.
15. E. J. MITTEMEIJER, A. B. P. VOGELS and P. J. van der SCHAAF, *Scripta Metall.* **14** (1980) 411.
16. C. DAWES, D. F. TRANTER and C. G. SMITH, *Metals Technol.* **6** (1979) 345.
17. K. H. JACK, *Proc. Roy. Soc. London* **208A** (1951) 216.

Received 3 February
and accepted 24 June 1983